Papers

Conformal mapping of the Gulf of Gdańsk onto a canonical domain

OCEANOLOGIA, 44 (2), 2002.
pp. 179–207.

KEYWORDS
Shoreline
Conformal mapping
Domain of solution
Computational domain
Inversion
Schwarz-Christoffel function
Inverse of a function

Paweł P. Cześnik
Włodzimierz J. Prosnak
Institute of Oceanology,
Polish Academy of Sciences,
Powstańców Warszawy 55, PL–81–712 Sopot, Poland;
e-mail: czesiek@iopan.gda.pl

Manuscript received 7 February 2002, reviewed 15 April 2002, accepted 8 May 2002.

Abstract

The paper deals with the conformal mapping of a plane, finite, simply connected domain, representing the southern segment of the Gulf of Gdańsk, enclosed from the North by a parallel, tangential to Cape Rozewie. The segment contains the Hel Peninsula.

The method of *double* decomposition, presented in Prosnak & Cześnik (2001), is applied to the transformation of such an *original* domain onto a *canonical* one, which consists of two separate unit discs.

The *first* decomposition concerns the domain which is split into two adjacent subdomains by means of a segment of a straight line.

The *second* decomposition involves two holomorphic functions, each one mapping a subdomain onto a separate disc. The decomposition consists in replacing the function by a sequence of simple ones, so that the mapping is performed step-wise. Each sequence starts with the *Schwarz-Christoffel* function, the last step consisting in an inversion that transforms an infinite circular domain onto a disc.

The data for the problem is contained in the Annex, and is represented by two sets of rectangular coordinates defining consecutive discrete points of the contours bounding the subdomains.

The solution to the problem consists of:

– two sets of functions, consecutively transforming each of the subdomains;
– the numerical values of the parameters of these functions;
– a set of figures illustrating the consecutive transformations.

The accuracy of the first, and of the penultimate transformation are given, because only in the case of these two functions do the unknown coefficients have to be determined by means of a suitable iterative process. The coefficients of all the remaining functions are evaluated from exact formulae.

It should be recalled that the depth of the Gulf of Gdańsk varies considerably – from a few to 110 metres – the gradients of the bottom being rather large. Therefore, the domain of the solution for any mathematical problem describing the hydrodynamical phenomena occurring in the Gulf is usually taken to be *three-dimensional*. Nevertheless, the paper deals with the transformation of the *free surface* of the Gulf, *assumed as plane*. It should be emphasized that this assumption does not mean that the whole domain of the solution has to be regarded as plane.

1. Motivation

There are two motives for undertaking, within the framework of this paper, the task of transforming the free surface of the Gulf of Gdańsk onto a canonical domain consisting of two separate unit discs.

The first motive stems from our wish to obtain a convenient, universal 'battle field' for several partial differential problems describing various flows in the Gulf, problems that differ with respect to their physical models, and, consequently, in the sets of differential equations as well as in the boundary and initial conditions. It is hoped that arriving at the solutions of all such problems may be simplified and systematized if all domains of solutions possess a common feature, represented by a *regular* free surface consisting of discs.

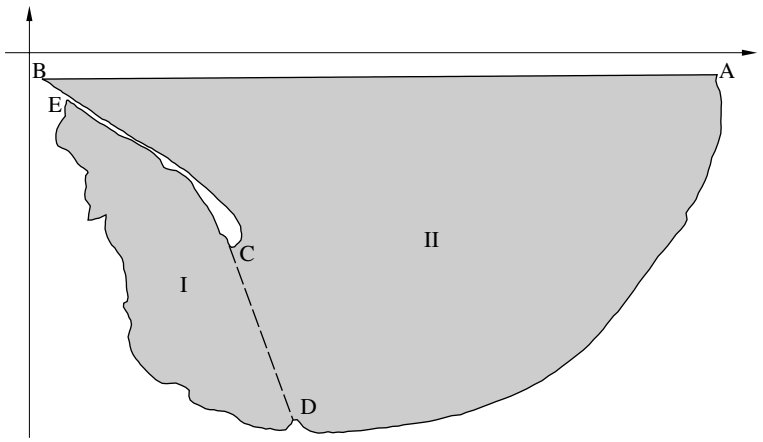

Fig. 1. The part of the Gulf of Gdańsk considered, and its decomposition into two subdomains

The second motive stems from our intention to check whether the method of transformation published earlier in Prosnak & Cześnik (2001) could also be applied to domains with deep indentations, such as the Hel Peninsula (Fig. 1).

The method to be applied in the paper is based on two kinds of decomposition. The first one involves decomposition of the given, *original* domain into subdomains, which are then transformed independently onto discs. The second kind of decomposition concerns every mapping function which performs a conformal transformation of a single subdomain. The function is regarded as a sequence of simple auxiliary mapping functions, performing *step-by-step* the transformation of the subdomain under consideration onto the unit disc.

Application of the method to the domain representing the Vistula Lagoon (Prosnak & Cześnik 2001) yielded quite satisfactory results. It is obvious, however, that this solitary success does not suffice to formulate general conclusions as far as the method is concerned. Further applications, differing in geometrical shape of the domains, are needed for this purpose.

2. Definition of the primitive domain

The plane, finite, simply connected domain considered in this paper (Fig. 1) represents the free surface of the Gulf of Gdańsk, bounded by the shoreline, and – in the North – by a parallel, tangential to Cape Rozewie.

Such a definition of the domain can be found in Druet & Jankowski (1983).

The domain has to be defined by discrete points distributed along its boundary.

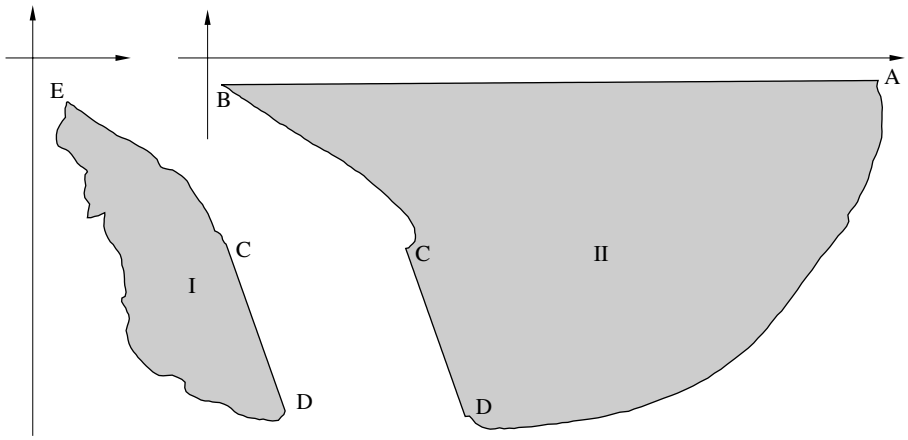

Fig. 2. The two subdomains shown separately

We have prepared the set of such points with the aid of the map published in Ciołkosz & Ostrowski (1995), which is based on satellite photographs. The number of points defining the segment of the shoreline is equal to 334. There are 100 points distributed on the parallel. Finally, the dashed rectilinear segment (Fig. 1) dividing the domain into two subdomains, is defined by means of 50 equidistant points. Eventually, the numbers of the points defining the two contours shown in Fig. 2 turn out to be 227 and 310 respectively. The values of the rectangular coordinates of these points are set out in the Annex, for each subdomain separately.

The five characteristic points A, B, C, D, E denoted in Figs. 1 and 2 can be identified by means of the numbers contained in the Tables, namely:

A – No. 209 in Table A-II

B – No. 1 in Table A-II

C – No. 63 in Table A-II, and No. 1 in Table A-I

D – No. 114 in Table A-II, and No. 176 in Table A-I

E – No. 56 in Table A-I.

The sets of points defining the boundaries of the subdomains are stored in the files ZGNpuck.dan and ZGNgda.dan – as indicated in the Annex.

3. The background of the method of transformation

The method of transformation applied in this paper is identical with the one introduced in Prosnak & Cześnik (2001), where the general features of the method as well as its most important details are presented. Nevertheless, for the sake of completeness they should be briefly recalled in this section.

3.1. Existence, univalence and standard representations of the mapping functions

Let us consider in the complex z-plane a given *finite*, simply connected domain, bounded by a *Jordan* curve. Let us consider also – in another complex plane denoted ζ – a disc with a given radius A. The theory of conformal mapping ensures the existence and univalence of a holomorphic function

$$z = f_{\text{in}}(\zeta), \tag{1}$$

which conformally transforms the disc onto the given domain.

The theory also ensures that the mapping function (1) can always be represented by the power series

$$z = f_{\text{in}}(\zeta) = \sum_{n=0}^{\infty} C_n \left(\frac{\zeta}{A}\right)^n, \tag{2}$$

where

$$C_n; \qquad n = 0, 1, 2, ... \tag{3}$$

stand for complex coefficients of the series. If $A = 1$, then the disc is called the *unit disc*. The series (2) is convergent in the whole disc as well as on the bounding circle. The series (2) will be called the *standard* form of the function (1) in further considerations.

Analogous properties concern an *infinite*, simply connected domain, represented by the whole z-plane with a cut-out, also bounded by a *Jordan* curve. In this case, the *standard* mapping function has the following form:

$$z = f_{\text{ex}}(\zeta) = G_{-1}\zeta + \sum_{n=0}^{\infty} G_n \left(\frac{a}{\zeta}\right)^n, \tag{4}$$

where a denotes the radius of the circle, bounding the 'hole' in the ζ-plane. The symbols

$$G_n; \qquad n = -1, 0, 1, 2, 3, ... \tag{5}$$

denote complex coefficients of the series (4), the series being convergent in the whole, simply connected, infinite exterior of the circle, and on the circle itself. It should be recalled that the point $\zeta = \infty$ belongs to the ζ-domain as well as the circle. Its image $z = \infty$ belongs, consequently, to the z-plane as well as the *Jordan* curve.

3.2. General remarks on the determination of the coefficients

Effective conformal mapping of the interior or exterior of the circle onto a given corresponding domain may be thought of as determination of the complex coefficients (3) or (5), respectively. Unfortunately, the theory of conformal mapping disappoints us at this crucial point: it does not deliver a general algorithm performing this task for domains of arbitrary shapes. True, such algorithms do exist, but as a rule they work satisfactorily only for particular classes of domains, e.g. for the exteriors of airfoil sections.

We will confine ourselves in the further considerations to two algorithms for determining coefficients (3) and (5), respectively, developed by ourselves, and published in Prosnak & Klonowska (1996). The experience with the application of these algorithms leads to the following conclusions.

I. The series (4) pertaining to *infinite* domains converge – under comparable conditions – more quickly than the series (2), which pertain to *finite* domains. Moreover, the same accuracy of mapping may be obtained with fewer coefficients.

II. Both the series (2) and (4) are unsuitable for describing boundaries possessing discontinuities of the tangent. In such cases a large number of terms in the corresponding series has to be retained in order to

obtain sufficient accuracy of the mapping. Moreover, the convergence is usually poor, and very often the series diverge. Cusps pointing towards the outside of the domain are particularly difficult in this respect.

III. Determination of coefficients (3) of the series (2) is rather troublesome in cases where the domain is elongated. Again, a large number of terms must be retained, which may lead to unacceptable numerical errors. On the other hand, determination of the coefficients (5) is equally easy (or equally difficult) for *elongated boundary contours* as well as for the ones not differing too much from a circle.

The conclusion to be drawn from these facts is very simple: the efforts to determine 'by force' the coefficients (3) or (5) for geometrically rather complicated shorelines, characteristic of natural bodies of water, are pointless. 'By force' means here 'by retaining more and more terms' in the series.

The theoretical explanation of the behaviour presented in I, II, III is fairly obvious, and will be left aside.

In any case, the need arises for a means of circumventing the difficulties just outlined.

The general idea of such a means has already been presented in our earlier paper (Prosnak & Cześnik 2001): it consists precisely of two kinds of **decomposition**.

The *first kind* is applied to a given **finite** domain, which is replaced – by means of suitable cuttings – by a sum of subdomains, every one of them being geometrically simpler than the originally given one. This means that the boundary line of any subdomain approximates a circle better than the given one. A typical example of such a decomposition is shown in Figs. 1 and 2.

Next, every subdomain is regarded as entirely separate from the remaining ones, and a complex mapping function is sought which transforms a disc onto the selected subdomain. Assuming that the subdomain and the disc are located in complex planes z and ζ, respectively, the general form of the unknown mapping function can be written as

$$z = f(\zeta). \tag{6}$$

The function, inverse with respect to (6), i.e.:

$$\zeta = f^{-1}(z) = F(z) \tag{7}$$

will be also taken into account in further considerations.

Usually, the subdomain is still too complicated geometrically – in order to be transformable *directly* onto the interior or exterior of a circle – by means of the series (2) or (4), respectively. Hence, the task of

determining the function (7) has to be performed step-wise. In other words – it has to be decomposed. In such a manner one arrives at the *second kind* of decomposition, which – unlike the first kind – consists in determining a set of *intermediate* transformations:

$$\zeta_1 = F_1(z); \qquad \zeta_2 = F_2(\zeta_1); \qquad ...; \qquad \zeta = F_K(\zeta_{K-1}), \tag{8}$$

where successive approximations of the considered subdomain appear in the complex planes:

$$\zeta_1; \qquad \zeta_2; \qquad ...; \qquad \zeta_{K-1}; \qquad \zeta. \tag{9}$$

It should be understood that the considered subdomain belongs to the z-plane, and the disc – to the ζ-plane.

In the present paper it is assumed that all functions (8) except two are represented by simple, exact formulae, containing complex constants, which are either known, or can be evaluated from known relations. One of the two remaining functions is represented by the series (4), and its unknown coefficients have to be determined by means of the iterative process governed by the algorithm published in Prosnak & Klonowska (1996). The second one of the two functions is identical with the *Schwarz-Christoffel* function (Prosnak & Cześnik 2001), and it will be recalled in the next subsection.

The remaining, *exact* auxiliary mapping functions are discussed in Prosnak & Cześnik (2001), and the reader is referred to this source. In any case, the functions are very simple, and they consist mainly in shifting, turning, and scaling of the considered intermediate subdomain as well as of its inversion. Also the *Joukowski* and the *Kármán-Trefftz* functions are exact intermediate functions. They will be not recalled – for the sake of brevity.

Just one of the auxiliary functions was not presented in our former paper (Prosnak & Cześnik 2001): it corresponds to the simple problem, illustrated in Fig. 3, which can be formulated as follows.

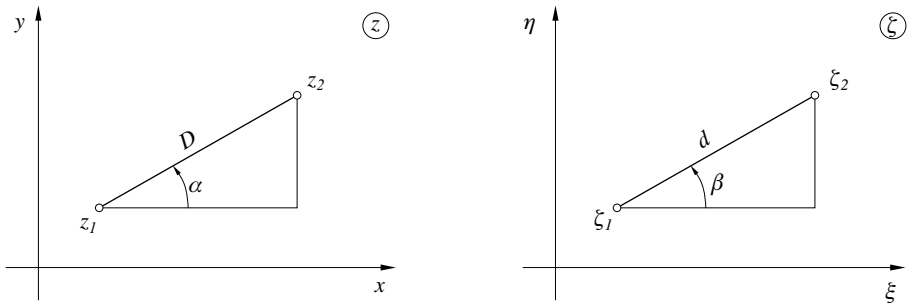

Fig. 3. Transforming a chord (z_1, z_2) into a given one (ζ_1, ζ_2)

Two points – z_1 and z_2 – of a domain situated in the complex z-plane are given. A formula is sought to transform the domain – by the use of shifting, turning and scaling – into another one which is located in the ζ-plane in such a manner that the segment $(z_1,\ z_2)$ maps into another one $(\zeta_1,\ \zeta_2)$, which is also given.

By introducing the auxiliary notation

$$D = |z_2 - z_1|; \qquad \alpha = \mathrm{Arg}(z_2 - z_1);$$

$$d = |\zeta_2 - \zeta_1|; \qquad \beta = \mathrm{Arg}(\zeta_2 - \zeta_1),$$

one can easily arrive at the relation

$$\zeta_2 - \zeta_1 = W(z_2 - z_1),$$

where

$$W = \frac{d}{D} e^{i(\beta - \alpha)}.$$

Hence, the sought-for image ζ of an arbitrary point z will be given by the formula

$$\zeta = \zeta_1 + W(z - z_1). \tag{10}$$

Subdomains transformed by means of (10) can easily be made to comply with subroutines for the auxiliary functions of *Joukowski* and *Kármán-Trefftz*.

3.3. The set of functions performing the step-wise transformation of a finite subdomain

In order to simplify the references, which will be used in the description of the step-wise transformation of any one of the two subdomains shown in Fig. 2, the corresponding formulae for the functions, representing consecutive steps of the transformation, will be recollected in the present subsection. Explanations of the formulae will be as concise as possible, the reader interested in details being referred to Prosnak & Cześnik (2001) and to Prosnak & Klonowska (1996).

(1) The *Schwarz-Christoffel* function

$$z = K_0 + K_1 \int_{\zeta_d}^{\zeta} \prod_{n=1}^{N} \left(1 - \zeta e^{-i\theta_n}\right)^{p_n} d\zeta \tag{11}$$

conformally maps the closed unit disc onto the closed interior of a given polygon containing N vertices, which are defined by means of the given complex numbers:

$$z_1, \qquad z_2, \qquad ..., \qquad z_N. \tag{12}$$

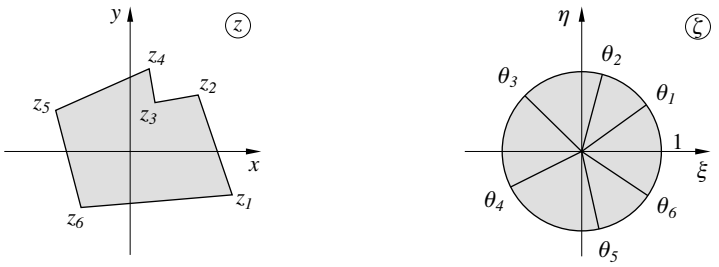

Fig. 4. Conformal mapping of a disc onto the interior of a polygon

The exponents p_n depend on the inner angles α_n of the polygon:

$$p_n = \frac{\alpha_n}{\pi} - 1; \qquad n = 1, 2, ..., N, \tag{13}$$

and have to be considered as known. The remaining exponents:

$$\theta_n; \qquad n = 1, 2, ..., N \tag{14}$$

represent images of the vertices on the circle bounding the unit disc, and are referred to as *parameters* of the *Schwarz-Christoffel* function (11). In the case of regular polygons they can be evaluated very easily. Otherwise, they have to be determined as a solution of a nonlinear 'parameter problem' by means of an iterative process (Prosnak & Klonowska 1996). The function (11) can be developed into a series:

$$z = \sum_{k=0}^{K} B_k \zeta^k, \tag{15}$$

where the coefficients B_k depend *explicitly* on the constants of (11) – in particular on the *parameters* (14). The respective relations have been derived in the book just cited.

The inverse of the function (15) can be written formally as

$$\zeta = \sum_{k=0}^{K} \tilde{B}_k z^k. \tag{16}$$

It plays an important role as one of the auxiliary functions (8). In the present paper as well as in the previous one (Prosnak & Cześnik 2001) it is evaluated as a numerical solution of (15) with respect to ζ, so that computation of the coefficients $\tilde{B}$ is not necessary.

(2) The *Joukowski* function

$$z = \zeta + \frac{c^2}{\zeta}; \qquad c - \text{real} \tag{17}$$

transforms circles onto ellipses or onto so-called *Joukowski* profiles. Very often, the function

$$\zeta = \frac{z}{2} \pm \sqrt{\left(\frac{z}{2}\right)^2 - c^2}, \tag{18}$$

inverse with respect to (17), is applied. The *Joukowski* profiles possess one or two cusps, characterized by the angle $\delta = 0$ between tangents.

Only two particular forms of the *Joukowski* profile have been applied in calculations pertaining to the present paper, viz. the rectilinear segment, and the arc of the circle. These two cases will be distinguished in further considerations by means of the indices s or a, respectively, following the symbol of the *Joukowski* function – see Tables 2, and 4.

(3) The *Kármán-Trefftz* function

$$\frac{z - 2c}{z + 2c} = \left(\frac{\zeta - c}{\zeta + c}\right)^m; \qquad 0 < m < 2; \qquad c - \text{real}, \tag{19}$$

represents a generalization of (17). It reduces to this particular function when $m = 2$. The relation between the exponent m and the angle δ at the cusp between the two tangents has the following form:

$$m = \frac{2\pi - \delta}{\pi}. \tag{20}$$

For $m = 2$, the angle δ at the cusp is equal to zero. For $m = 0$, the angle δ equals 2π.

More exactly, the profile is *convex* (see Fig. 7 – left) or 'indented' (see Fig. 13 – left), if

$$0 < \delta \leq \pi; \qquad \pi < \delta \leq 2\pi,$$

respectively.

The *Kármán-Trefftz* function is applied in the present paper for the task of 'unbending' the boundary of the considered domain. Such 'unbending' may also be necessary in the case when – instead of the cusp – a very large curvature of the contour appears.

(4) *Inversion* is defined by means of the following function:

$$z = \frac{1}{\zeta} \tag{21}$$

or by its inverse:

$$\zeta = \frac{1}{z}. \tag{22}$$

It is usually applied to transform a finite domain onto an infinite one or vice versa – in order to enable one to use the series (4) instead of (2) – in such a particular step of the whole set of consecutive mappings, which corresponds to the transformation of the contour bounding the approximate domain onto a circle. The advantage stemming from such an approach was explained in the previous subsection.

(5) Turning the contour by the angle α:

$$z = \zeta e^{i\alpha}; \qquad \alpha - \text{real}. \tag{23}$$

(6) Shifting the contour:

$$z = c + \zeta; \qquad c - \text{complex}. \tag{24}$$

(7) Scaling the contour:

$$z = c\zeta; \qquad c - \text{real}. \tag{25}$$

(8) Locating a given chord of the contour into a desired position is performed by means of the function (10), and will be referred to by the use of this symbol.

It should be stressed that – besides the functions (10)–(25), each one corresponding to a single step of the whole mapping (6) – some *operations* usually have to be performed which stem from the following properties of the boundary of the domain:

I. The boundary is defined by means of separate points which are numbered consecutively, starting from a properly selected one. The results of such definitions are given in Tables A-I and A-II.

II. The boundary represents a *contour*. Therefore, the direction assumed on the boundary has to comply with the direction in which numbers of the consecutive points increase.

The *first operation* consists in changing the number of the first point of the contour, and as a consequence, 'renumbering' the remaining ones. It will be referred to as

changing the origin. (26)

The direction of the contour is not changed during this operation.

On the other hand, if the direction of a contour is reversed, which happens as a 'by-product' of inversion, the proper direction has to be restored. This *second operation* will be referred to as:

changing the direction. (27)

Suitable procedures of the computer programs perform both operations (26), (27) automatically – for values of parameters introduced by the user from the keyboard.

4. Results of conformal mapping of the Gulf of Gdańsk

The results consist of two parts, corresponding to two subdomains, denoted I and II in Figs. 1 and 2. In accordance with the applied method, each domain is transformed independently of the other one. Consequently, the results are presented in two independently subsections.

Each subsection contains three elements pertaining to the applied computer programs.

The first element consists of a Table containing values of vertices, and the parameters of a polygon circumscribing the domain under consideration. The parameters represent the solution of the corresponding *parameter problem* for the *Schwarz-Christoffel* function. The values of the errors are given in the Table, too.

The parameter problem is solved by means of the program denoted B_II_5n.pas. The same program applies the function, inverse with respect to (15), and denoted (16) – to transform an original subdomain onto one circumscribed by the unit circle.

The second element of any one of the two following subsections consists of another Table, which contains the list of functions and operations describing consecutively all the *auxiliary* transformations of the subdomain. The Table has been prepared by means of the program VisBay78. One row of the Table refers to a single transformation, which is indicated by its symbol, and by the symbols ζ_n, ζ_{n+1} of two complex planes that contain the subdomain before and after the transformation, respectively. Some of the transformations are illustrated by means of Figures, each one showing two such consecutive approximations of the subdomain under consideration. The Table starts with the approximation, representing the finite subdomain, circumscribed by the unit circle, as shown on the right-hand side of Fig. 5. It terminates with the infinite one, which will be dealt with by the program VE2.pas.

Hence, the third element of the subsection contains final transformations and results, delivered by the program just mentioned, which performs the following tasks.

I. Conformal mapping of the last, approximate, infinite domain, onto the infinite exterior of a circle; this task reduces to the determination of the radius a of the circle as well as of the coefficients (5) of the function (4).

II. Inversion (21) of the exterior thus obtained onto the quasi-disc.

III. Rescaling of this result in order to arrive at a contour resembling the unit circle.

IV. Change of direction (27) of the contour, i.e. ascribing new numbers to the points defining the contour. The results contain values of the coefficients (5); the data applied for arriving at these values is also given. The final result, however, is presented in graphical form.

It shows the unit circle as well as the contour delivered by the program VE2.pas. The difference between these two lines illustrates the cumulative error of the whole set of consecutive conformal mappings.

4.1. Subdomain No. 1

Subdomain I, shown in Figs. 1 and 2, is rotated by means of the function (23) through the angle $\alpha = -30^\circ$, and a nonagon is selected, circumscribing the so-turned subdomain. The situation is illustrated at the left-hand side of Fig. 5, wherein the subdomain is shaded, and the nonagon is denoted by means of the thin solid line.

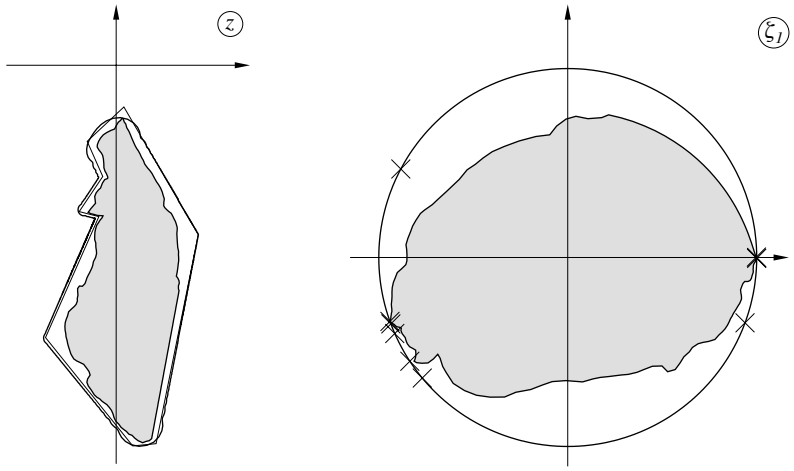

Fig. 5. Transforming of the initial subdomain No. 1 by means of the series (16), which is inverse with respect to the series (15), stemming from the development of the *Schwarz-Christoffel* function (11)

The third contour visible in this Figure represents the *approximate* nonagon, calculated by means of the function (15), which represents the development of the *Schwarz-Christoffel* function (11) into a series. Only $K = 150$ terms have been retained in the series.

Rectangular coordinates of the vertices of the nonagon as well as solution to the corresponding parameter problem are given in Table 1. The errors of the solution refer to the ratios of consecutive sides of the polygon and its circumference. They are defined as the differences between two ratios corresponding to the given polygon and to its approximation, respectively.

The relatively small errors concerning the parameters are worthy of notice.

Table 1. Vertices and parameters of the nonagon

n	1	2	3	4	5
x_n	0.1500	0.0160	–0.0500	–0.0220	–0.0644
y_n	–0.3000	–0.0700	–0.1320	–0.1951	–0.2583
θ_n	152.1°	199.8°	200.6°	203.7°	213.3°
error	-3.2×10^{-4}	-6.3×10^{-5}	-1.7×10^{-4}	-7.9×10^{-4}	-7.8×10^{-4}
n		6	7	8	9
x_n		–0.0289	–0.1250	0.0320	0.0740
y_n		–0.2674	–0.4850	–0.6800	–0.6760
θ_n		219.7°	339.8°	359.7°	0.0°
error		-7.3×10^{-4}	-1.2×10^{-3}	-2.3×10^{-3}	1.1×10^{-16}

It should be stressed that the number of vertices, and their positions with respect to the considered subdomain, depend on the researcher.

The result of transformation of the shaded domain, shown in the left-hand-side of Fig. 5, and obtained by means of the inverse (16) with respect to the series (15), appears in the right-hand side of this Figure. The circle represents the *exact* counter-image of the nonagon: it could be determined only by means of *exact* inversion with respect to the function (11).

The consecutive approximate subdomains are listed in Table 2. Some of them are illustrated by means of Figures 6–9. The symbols L and H in the Table define the arc to be transformed into the 'full' circle. The fundamental transformation of the finite subdomain onto the infinite one is shown in Fig. 6.

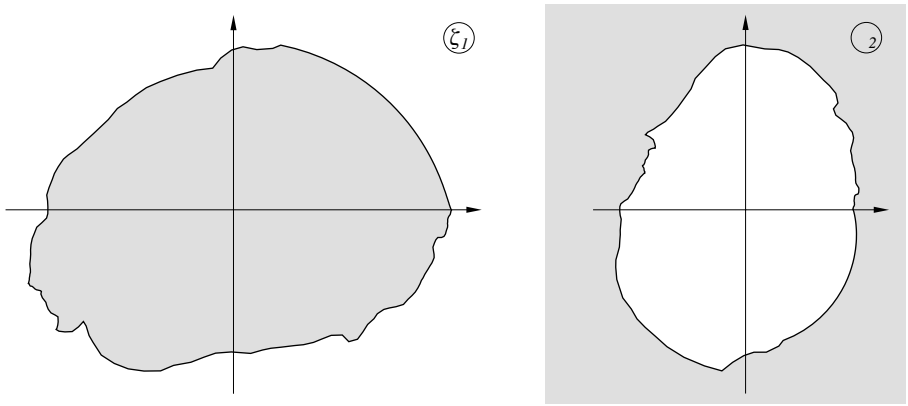

Fig. 6. Transformation of the finite domain onto the infinite one by means of inversion (22)

Table 2. List of consecutive transformations of subdomain No. 1

No.	Function or operation	Complex planes independent	Complex planes dependent	Given values of parameters	Figure
1	inversion (22)	ζ_1	ζ_2	———	Fig. 6.
2	changing the direction (27)	———	———	———	———
3	changing the origin (26)	———	———	[133] = [1]	———
4	locating a chord (10)	ζ_2	ζ_3	[204,1]→[(–30,0), (2,0)]	———
5	turning the contour (23)	ζ_3	ζ_4	$\alpha = -0.8203488°$	———
6	shifting the contour (24)	ζ_4	ζ_5	[1]→(2,0)	———
7	*Kármán-Trefftz* function (19)	ζ_5	ζ_6	$\delta = 72.874598°$	Fig. 7.
8	locating a chord (10)	ζ_6	ζ_7	[94,6]→[(–200,0), (2,0)]	———
9	turning the contour (23)	ζ_7	ζ_8	$\alpha = 1.0350294°$	———
10	shifting the contour (24)	ζ_8	ζ_9	[6]→(2,0)	———
11	*Kármán-Trefftz* function (19)	ζ_9	ζ_{10}	$\delta = 273.4949638°$	———
12	changing the origin (26)	———	———	[211] = [1]	———
13	locating a chord (10)	ζ_{10}	ζ_{11}	[16,84]→[(–2,–0.6), (2,–0.6)]	———
14	*Joukowski* function $(18)_s$	ζ_{11}	ζ_{12}	———	Fig. 8.
15	locating a chord (10)	ζ_{12}	ζ_{13}	[213,224]→[(–1,–0.05), (1,–0.05)]	———
16	*Joukowski* function $(18)_a$	ζ_{13}	ζ_{14}	$L = 1.4$, $H = 0.2$	Fig. 9.
17	locating a chord (10)	ζ_{14}	ζ_{15}	[16,33]→[(–1,–0.05), (1,–0.05)]	———
18	*Joukowski* function $(18)_a$	ζ_{15}	ζ_{16}	$L = 1.6$, $H = 0.4$	———
19	locating a chord (10)	ζ_{16}	ζ_{17}	[105,3]→[(–0.5,0), (0.5,0)]	———
20	changing the origin (26)	———	———	[3] = [1]	———

Application of the *Kármán-Trefftz* function (19) to the local unbending of the contour can be seen in Fig. 7.

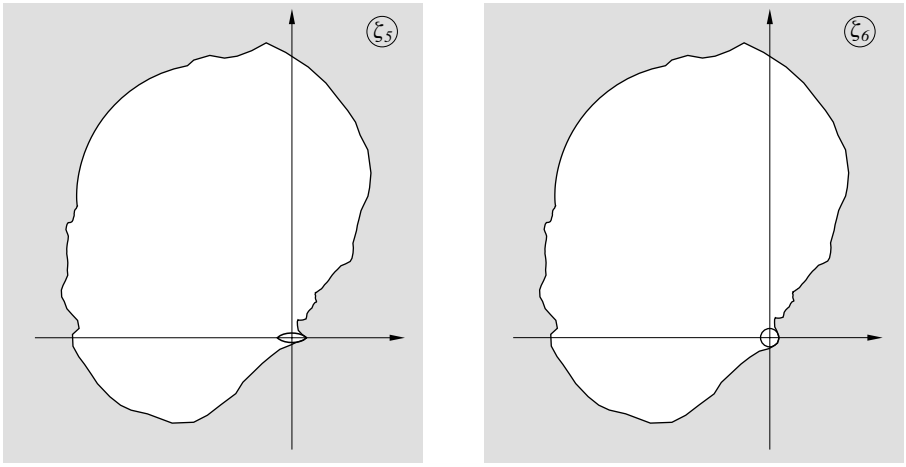

Fig. 7. Unbending by means of the *Kármán-Trefftz* function (11)

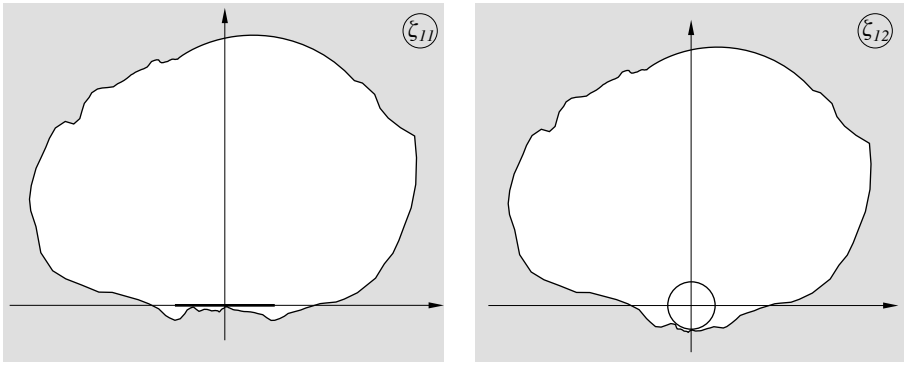

Fig. 8. Stretching by means of the *Joukowski* function (18)

Figures 8 and 9 show local 'rectifications' of the contour, performed by means of the *Joukowski* function (17).

The final element of the transformations applied to the subdomain No. 1 is shown in Fig. 10. The unit circle is denoted in the Figure by means of the dashed line.

The quasi-disc corresponding to the subdomain is bounded by the solid line, and its interior is shaded. The maximal distance between the two lines, i.e. the cumulative error of the set of transformations Er = 0.0058.

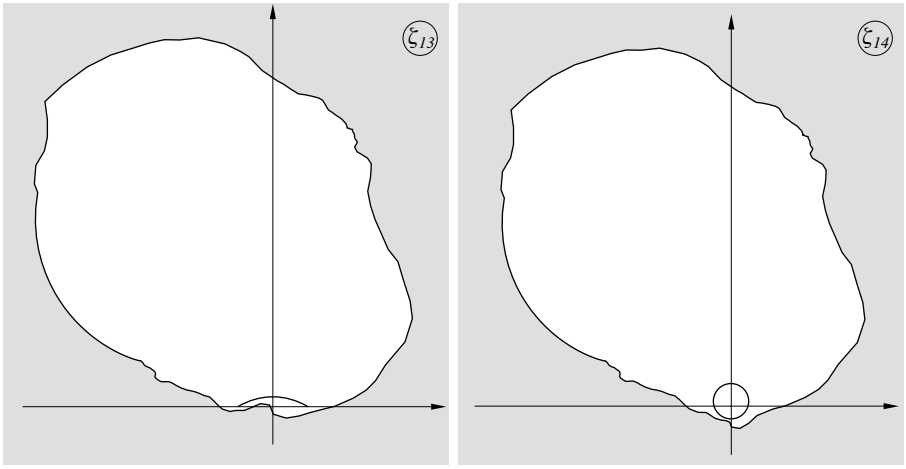

Fig. 9. Unbending by means of the *Joukowski* function (18)

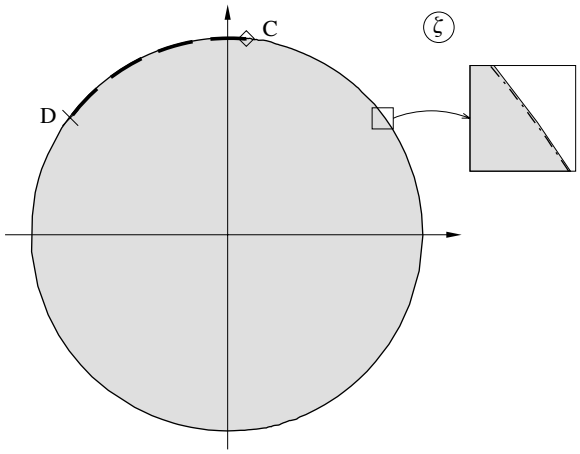

Fig. 10. Final result: the unit disc representing subdomain No. 1

One rather important detail of the computations should be mentioned. It concerns the determination of the constants of the standard function (4). The relevant data are

$$N = 198; \qquad m = 1000; \qquad prec = 10^{-9}; \qquad it = 30, \tag{28}$$

where N denotes the number of terms in the series; m – number of nodes appearing during integration; $prec$ – index of 'accuracy', controlling the termination of the iterative process; it – number of iterations. The numerical values of the coefficients

$$a; \qquad G_n; \qquad n \in [-1, 198] \tag{29}$$

are not included in the present paper for the sake of conciseness. However, they can be obtained from the first author, at the Institute of Oceanology PAS.

4.2. Subdomain No. 2

The preliminary transformation of the subdomain, denoted by the number II in Figs. 1 and 2, involves the application of the function (10) to the points numbered 1 and 209 in Table A-II. These points are translated to the following ones:

$$(-0.5, 0.2) \qquad (0.5, 0.2). \tag{30}$$

The result can be seen on the left-hand-side of Fig. 11.

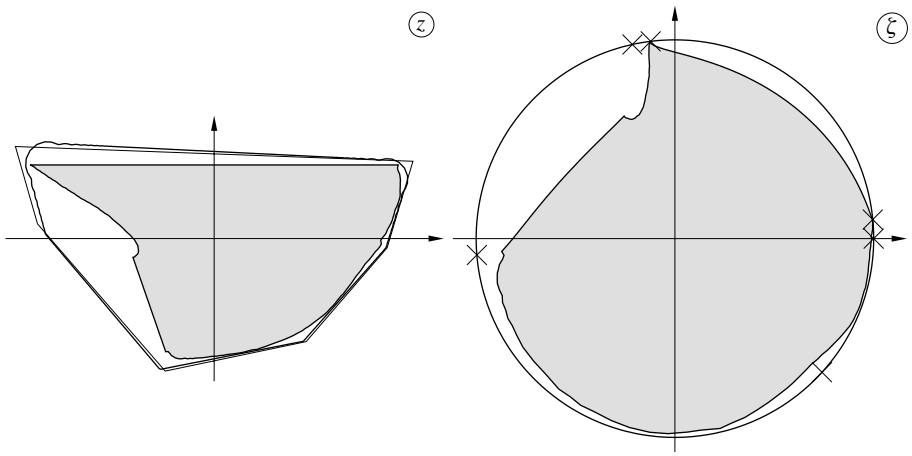

Fig. 11. Transforming the initial subdomain No. 2 by means of the series (16), which is inverse with respect to the series (15), stemming from the development of the *Schwarz-Christoffel* function (11)

Similarly, as in the former subsection, a hexagon is selected, circumscribing the domain, as shown in Figure just referred to. Vertices, and parameters of the hexagon are collected in Table 3.

Table 3. Vertices and parameters of the hexagon

n	1	2	3	4	5	6
x_n	0.540	–0.540	–0.480	–0.133	0.250	0.470
y_n	0.210	0.250	0.040	–0.360	–0.280	–0.025
θ_n	5.5°	97.0°	102.4°	184.7°	317.7°	0.0°
error	-4.0×10^{-4}	-6.3×10^{-3}	3.8×10^{-4}	-2.5×10^{-3}	-1.0×10^{-3}	-2.2×10^{-16}

This fundamental result does not need any comment: it is wholly analogous to Table 1.

The domain, representing the transformation of the domain located inside the polygon, is shown on the right-hand-side of Fig. 11 together with its circumscribing circle. As before, the finite domain so obtained is transformed into an infinite one by means of inversion (21), as illustrated in Fig. 12.

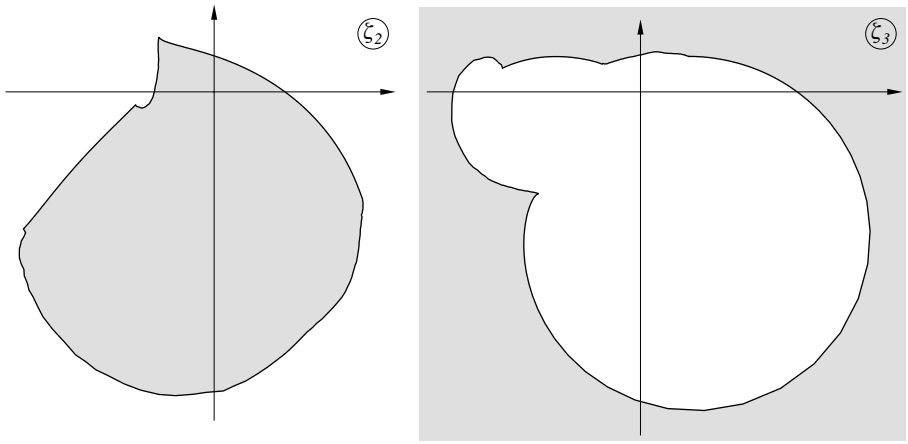

Fig. 12. Transformation of the finite domain onto the infinite one by means of inversion (22)

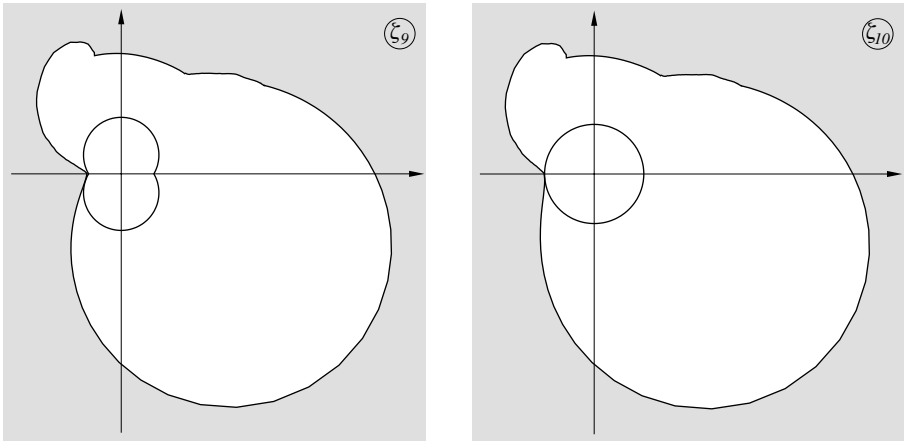

Fig. 13. Local rectification by means of the *Kármán-Trefftz* function (19)

The consecutive transformations yielding more and more regular approximations of the subdomain under consideration are collected in Table 4.

Table 4. List of consecutive transformations of subdomain No. 2

No.	Function or operation	Complex planes		Given values of parameters	Figure
		independent	dependent		
1	shifting the contour (24)	ζ_1	ζ_2	[1]→(–0.3, 0.3)	———
2	inversion (22)	ζ_2	ζ_3	———	Fig. 12.
3	changing the direction (27)	———	———	———	———
4	locating a chord (10)	ζ_3	ζ_4	[1,50]→[(–2,0), (150,0)]	———
5	turning the contour (23)	ζ_4	ζ_5	$\alpha = 5°$	———
6	shifting the contour (24)	ζ_5	ζ_6	[1]→(–2,0)	———
7	*Kármán-Trefftz* function (19)	ζ_6	ζ_7	$\delta = 320°$	———
8	turning the contour (23)	ζ_7	ζ_8	$\alpha = -5°$	———
9	shifting the contour (24)	ζ_8	ζ_9	[1]→(–2.1,0)	———
10	*Kármán-Trefftz* function (19)	ζ_9	ζ_{10}	$\delta = 240°$	Fig. 13.
11	locating a chord (10)	ζ_{10}	ζ_{11}	[270,248]→[(–50,0), (2,0)]	———
12	turning the contour (23)	ζ_{11}	ζ_{12}	$\alpha = 0.21838558°$	———
13	shifting the contour (24)	ζ_{12}	ζ_{13}	[248]→(2,0)	———
14	*Kármán-Trefftz* function (19)	ζ_{13}	ζ_{14}	$\delta = 277.8985515°$	———
15	locating a chord (10)	ζ_{14}	ζ_{15}	[27,264]→[(–2,0.52), (2,0.52)]	———
16	*Joukowski* function $(18)_s$	ζ_{15}	ζ_{16}	———	Fig. 14.
17	locating a chord (10)	ζ_{16}	ζ_{17}	[262,43]→[(–0.5,0), (0.5,0)]	———
18	changing the origin (26)	———	———	[43] = [1]	———

Some of them are illustrated by means of the corresponding Figures, e.g., the unbending of a contour by means of the *Kármán-Trefftz* function (19) is shown in Fig. 13. Similarly, application of the *Joukowski* function (17) in order to remove an indentation of the contour is shown in Fig. 14.

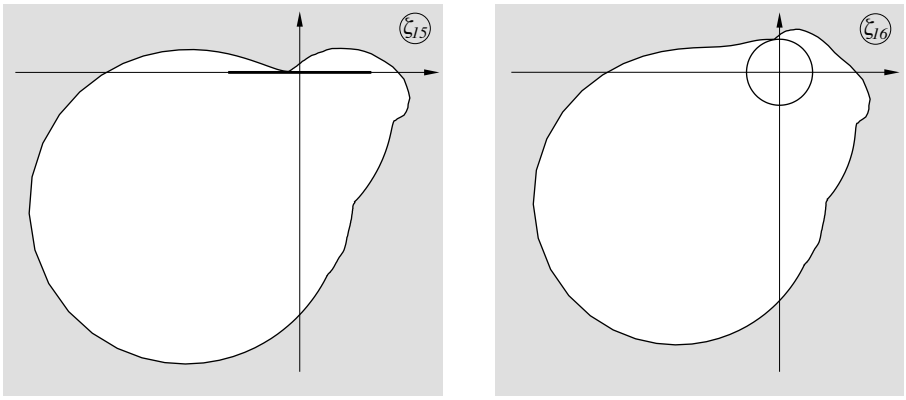

Fig. 14. Stretching by means of the *Joukowski* function (18)

The final result of the set of transformations, presented in this subsection, is shown in Fig. 15.

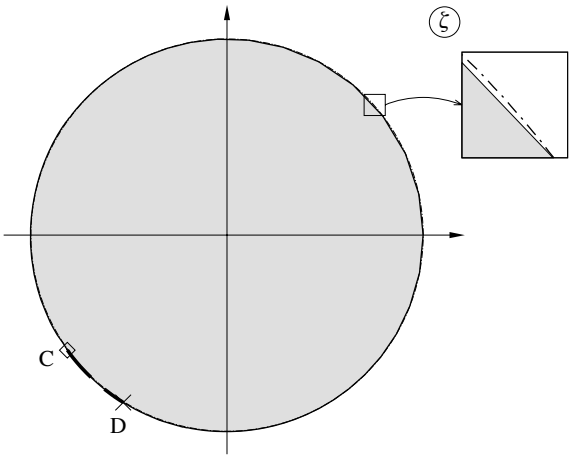

Fig. 15. Final result: the unit disc in the ζ-plane

As in Fig. 10, the unit circle is shown by means of the dashed line. The contour of the quasi-disc is denoted by means of the solid line, and its interior is shaded. The maximal cumulative error of the transformation Er = 0.0050, i.e. even slightly less than in the case of subdomain No. 1.

The data concerning the intermediate mapping function (4), analogous to (28), consist of the following numbers:

$$N = 198; \qquad m = 1000; \qquad prec = 10^{-8}; \qquad it = 25. \tag{31}$$

The constants of this function, like (29), are also available at the Institute of Oceanology, from the first author.

5. Comments

I. Three computer programs, designated B_II_5n.pas, VisBay78 and VE2.pas, were used in order to arrive at the presented results. The first one solves the parameter problem of the *Schwarz-Christoffel* function, and was borrowed from Prosnak & Klonowska (1996). All three programs can be obtained by e-mail from the first author of this paper.

The computer program VisBay78 is written in *Delphi*. Therefore, the structure of its name differs from that of the other two programs – B_II_5n.pas and VE2.pas – which are written in *Borland Pascal*.

Data for the latter two programs have to be introduced by the user from the keyboard. Afterwards, the programs run automatically from start to finish.

On the other hand, the program VisBay78 is designed as a 'conversational' one. It needs continual intervention on the part of the user, who has to determine again and again the kinds of consecutive transformations, and the values of the pertinent parameters.

II. In order to avoid any misunderstanding, it should be emphasized again that confinement of our considerations to a transformation of the *plane* domain, representing the water level of the Gulf of Gdańsk, definitely does not mean that the domain of a solution to a problem posed in the Gulf also has to be plane. Such a restriction is neither meant nor implied in any way. It should be rather understood that the original, three-dimensional domain of the Gulf transforms into two circular cylinders with uneven bottoms – accordingly to the shape of the bottom of the Gulf.

III. Tables A-I and A-II, containing coordinates of discrete points which define the boundaries of the two subdomains may seem superfluous. However, without these data our results could not be checked by an independent researcher, either by the use of our method or of a different one, such as that by Driscoll (1996).

IV. It should be kept in mind that the two discs representing images of the subdomains remain interconnected. Namely, in the circumference

of each circle bounding the disc, an arc can be distinguished, which represents the image of the rectilinear segment (CD in Figs. 1 and 2) separating the subdomains. Hence, any point of the set defining *one* arc has its known, corresponding 'twin' which belongs to the set defining the *second* arc. This allows one to formulate – in the canonical domain consisting of the two discs – the necessary *continuity conditions* which will occur e.g. in differential problems posed in this domain.

V. The described conformal mapping is not aimed at the construction of grids. It has been derived rather with the application of analytical-numerical methods in view, where the grid does not appear at all. Nevertheless, after mapping the obtained discs onto squares, one can easily arrive at the rectangular grid, so convenient when a discrete method of solution has to be applied, in particular, the method of finite differences.

The additional transformation of the disc onto the square can be performed by a number of mapping functions, the obvious one being the *Schwarz-Christoffel* formula. In this case the solution of the parameter problem follows instantaneously from geometrical properties of the square – cf. (11).

References

Ciołkosz A., Ostrowski M., 1995, *Atlas of satellite photographs of Poland*, Inst. Geodezji i Kartografii, SCI-ART, Polskie Przedsiębiorstwo Wydawnictw Kartograficznych im. E. Romera, S.A., Warszawa.

Driscoll T. A., 1996, *A MATLAB toolbox for Schwarz-Christoffel mapping*, ACM Trans. Math. Soft., 22, 168–186, (cited after Driscoll T. A., *Schwarz-Christoffel Toolbox User's Guide* available over the Web at http:/www.math.udel.edu/∼driscoll/SC/).

Druet Cz., Jankowski A., 1983, *Characteristics of hydrodynamic states and processes in the Baltic Sea induced by a uniform wind field*, [in:] *Fundamentals of economics in the marine environment*, Stud. i Mater. Oceanol., 40, 129–202, (in Polish).

Prosnak W. J., Cześnik P. P., 2001, *Transformation of the Vistula Lagoon onto a canonical domain*, Oceanologia, 43 (2), 169–200.

Prosnak W. J., Klonowska M. E., 1996, *Introduction to numerical fluid mechanics. Part B: conformal mapping*, Ossolineum, Wrocław, 998 pp., (in Polish).

Annex

Coordinates of discrete points which define the contours bounding the subdomains

Table A-I. Subdomain No. 1

file: ZGNpuck.dan; number of points: 227.

No.	x	y	No.	x	y
1	0.300200000000	–0.289300000000	50	0.084443939919	–0.090369830439
2	0.297775998661	–0.287405690250	51	0.078518049398	–0.085925412549
3	0.294813053401	–0.282467448150	52	0.072098334668	–0.082468643079
4	0.293825404981	–0.277529206049	53	0.067160092567	–0.077530400978
5	0.291356283930	–0.271109491318	54	0.062715674677	–0.075555104138
6	0.287405690250	–0.269134194478	55	0.058760000000	–0.071960000000
7	0.282961272360	–0.269134194478	56	0.057000000000	–0.071700000000
8	0.280985975519	–0.263208303958	57	0.056000000000	–0.072900000000
9	0.278023030259	–0.255800940807	58	0.055802135736	–0.076542752558
10	0.275060084999	–0.248887401866	59	0.053826838896	–0.081480994659
11	0.272590963949	–0.242961511345	60	0.053826838896	–0.088394533599
12	0.269628018688	–0.238023269245	61	0.054320663106	–0.095308072540
13	0.266665073428	–0.233578851354	62	0.049876245215	–0.100740138851
14	0.264195952378	–0.228640609254	63	0.045431827325	–0.107653677791
15	0.259257710277	–0.223208542943	64	0.041975057854	–0.114567216732
16	0.252837995546	–0.213825882952	65	0.040493585224	–0.121974579883
17	0.248393577656	–0.206912344012	66	0.040493585224	–0.128888118823
18	0.245430632396	–0.202467926121	67	0.041481233644	–0.135307833554
19	0.242467687135	–0.196048211391	68	0.043456530485	–0.139258427235
20	0.240492390295	–0.192591441920	69	0.048888596795	–0.142221372495
21	0.236047972405	–0.188147024030	70	0.055308311526	–0.144690493545
22	0.232097378724	–0.184690254559	71	0.059258905206	–0.147159614595
23	0.228146785044	–0.182221133509	72	0.063703323097	–0.152097856696
24	0.223208542943	–0.178764364039	73	0.068641565197	–0.159011395637
25	0.218270300843	–0.175801418778	74	0.072592158878	–0.165431110367
26	0.213825882952	–0.175307594568	75	0.077530400978	–0.169875528258
27	0.208887640852	–0.174319946148	76	0.080987170448	–0.171850825098
28	0.203455574541	–0.172838473518	77	0.086913060969	–0.176295242988
29	0.199998805071	–0.170863176678	78	0.087900709389	–0.178764364039
30	0.197035859811	–0.165431110367	79	0.084443939919	–0.183208781929
31	0.194566738760	–0.159505219847	80	0.083950115709	–0.190616145080
32	0.189134672450	–0.154566977746	81	0.085431588339	–0.199998805071
33	0.185184078769	–0.150616384066	82	0.083950115709	–0.204937047171
34	0.179258188249	–0.146171966175	83	0.082962467289	–0.211356761902
35	0.173332297728	–0.142715196705	84	0.083950115709	–0.218270300843
36	0.166912582997	–0.139752251445	85	0.088394533599	–0.224196191363
37	0.160986692477	–0.136295481974	86	0.091357478860	–0.228146785044
38	0.152591680906	–0.130863415664	87	0.089876006229	–0.235554148195
39	0.146665790385	–0.128394294613	88	0.088888357809	–0.240492390295
40	0.140739899865	–0.126418997773	89	0.088394533599	–0.246418280816
41	0.132838712504	–0.122962228303	90	0.087900709389	–0.248887401866
42	0.127406646193	–0.118517810412	91	0.093332775700	–0.248887401866
43	0.121480755673	–0.115061040942	92	0.099258666220	–0.246912105026
44	0.116048689362	–0.111110447262	93	0.104690732531	–0.245924456606
45	0.111110447262	–0.108147502001	94	0.109628974631	–0.243455335555
46	0.105678380951	–0.105678380951	95	0.114406623220	–0.241265668015
47	0.100246314640	–0.102221611481	96	0.114666048669	–0.244897624308
48	0.094814248330	–0.098271017800	97	0.113579568312	–0.250862698706
49	0.088888357809	–0.093826599910	98	0.113579568312	–0.254813292387

Coordinates of discrete points which define the contours bounding the subdomains (continued)

No.	x	y	No.	x	y
99	0.113085744102	–0.261726831327	151	0.244442983976	–0.519503068974
100	0.114567216732	–0.268146546058	152	0.251356522916	–0.522466014235
101	0.116542513572	–0.274072436579	153	0.256294765017	–0.524935135285
102	0.119505458832	–0.279998327099	154	0.261726831327	–0.527898080545
103	0.122962228303	–0.285924217620	155	0.268146546058	–0.529379553175
104	0.127406646193	–0.289874811300	156	0.274072436579	–0.529379553175
105	0.131357239874	–0.296294526031	157	0.279504502889	–0.530861025806
106	0.135307833554	–0.301232768131	158	0.284442744990	–0.531354850016
107	0.138270778814	–0.305677186022	159	0.290368635510	–0.531848674226
108	0.140246075655	–0.312590724963	160	0.297282174451	–0.534317795276
109	0.140739899865	–0.321479560744	161	0.302714240762	–0.536786916326
110	0.142715196705	–0.476046538490	162	0.308146307072	–0.540737510007
111	0.143702845125	–0.330862220735	163	0.313084549173	–0.545675752107
112	0.144196669335	–0.335800462835	164	0.319010439693	–0.549626345787
113	0.144690493545	–0.342714001776	165	0.326417802844	–0.551601642628
114	0.144690493545	–0.347158419666	166	0.332837517575	–0.554564587888
115	0.145184317755	–0.352590485977	167	0.339751056516	–0.555552236308
116	0.146171966175	–0.357034903867	168	0.344689298616	–0.556046060518
117	0.147159614595	–0.362960794388	169	0.351109013347	–0.558021357358
118	0.145678141965	–0.369380509119	170	0.357034903867	–0.557033708938
119	0.140739899865	–0.371849630169	171	0.363948442808	–0.559009005778
120	0.140246075655	–0.377281696479	172	0.371355805959	–0.559996654199
121	0.143209020915	–0.382219938580	173	0.380244641740	–0.559009005778
122	0.146665790385	–0.387158180680	174	0.384689059630	–0.553576939468
123	0.148641087226	–0.393084071201	175	0.388639653311	–0.550120169998
124	0.151110208276	–0.397034664882	176	0.390614950151	–0.544688103687
125	0.152097856696	–0.403454379612	177	0.388842107991	–0.539680493811
126	0.151110208276	–0.408392621713	178	0.387069265831	–0.534672883935
127	0.149134911436	–0.414318512233	179	0.385296423672	–0.529665274058
128	0.147159614595	–0.421725875384	180	0.383523581512	–0.524657664182
129	0.149134911436	–0.429133238535	181	0.381750739352	–0.519650054306
130	0.150122559856	–0.435552953266	182	0.379977897192	–0.514642444430
131	0.151604032486	–0.441478843786	183	0.378205055032	–0.509634834553
132	0.154566977746	–0.447898558517	184	0.376432212872	–0.504627224677
133	0.158517571427	–0.453824449037	185	0.374659370713	–0.499619614801
134	0.162468165107	–0.458268866928	186	0.372886528553	–0.494612004925
135	0.165431110367	–0.462713284818	187	0.371113686393	–0.489604395049
136	0.170369352468	–0.467651526919	188	0.369340844233	–0.484596785172
137	0.173826121938	–0.471602120599	189	0.367568002073	–0.479589175296
138	0.178270539829	–0.476046538490	190	0.365795159913	–0.474581565420
139	0.183208781929	–0.480490956380	191	0.364022317754	–0.469573955544
140	0.188147024030	–0.484935374271	192	0.362249475594	–0.464566345668
141	0.192097617710	–0.487404495321	193	0.360476633434	–0.459558735791
142	0.197529684021	–0.490367440581	194	0.358703791274	–0.454551125915
143	0.203949398751	–0.490861264791	195	0.356930949114	–0.449543516039
144	0.210862937692	–0.490367440581	196	0.355158106955	–0.444535906163
145	0.217776476633	–0.489873616371	197	0.353385264795	–0.439528296286
146	0.226171488204	–0.493330385842	198	0.351612422635	–0.434520686410
147	0.232591202934	–0.496293331102	199	0.349839580475	–0.429513076534
148	0.237529445035	–0.500737748992	200	0.348066738315	–0.424505466658
149	0.237035620825	–0.509132760563	201	0.346293896155	–0.419497856782
150	0.239010917665	–0.515058651084	202	0.344521053996	–0.414490246905

Coordinates of discrete points which define the contours bounding the subdomains (continued)

No.	x	y	No.	x	y
203	0.342748211836	–0.409482637029	216	0.319701263758	–0.344383708638
204	0.340975369676	–0.404475027153	217	0.317928421598	–0.339376098762
205	0.339202527516	–0.399467417277	218	0.316155579438	–0.334368488886
206	0.337429685356	–0.394459807401	219	0.314382737279	–0.329360879010
207	0.335656843196	–0.389452197524	220	0.312609895119	–0.324353269134
208	0.333884001037	–0.384444587648	221	0.310837052959	–0.319345659257
209	0.332111158877	–0.379436977772	222	0.309064210799	–0.314338049381
210	0.330338316717	–0.374429367896	223	0.307291368639	–0.309330439505
211	0.328565474557	–0.369421758019	224	0.305518526479	–0.304322829629
212	0.326792632397	–0.364414148143	225	0.303745684320	–0.299315219752
213	0.325019790238	–0.359406538267	226	0.301972842160	–0.294307609876
214	0.323246948078	–0.354398928391	227	0.300200000000	–0.289300000000
215	0.321474105918	–0.349391318515			

Table A-II. Subdomain No. 2

file: ZGNgda.dan; number of points: 310.

Coordinates of discrete points which define the contours bounding the subdomains (continued)

No.	x	y	No.	x	y
1	0.019752968402	–0.040493585224	29	0.169875528258	–0.136295481974
2	0.027160331553	–0.043950354695	30	0.176295242988	–0.140246075655
3	0.032098573653	–0.046913299955	31	0.182221133509	–0.142715196705
4	0.037530639964	–0.051851542055	32	0.187653199820	–0.146665790385
5	0.042468882064	–0.054814487316	33	0.193085266130	–0.149628735646
6	0.047900948375	–0.057777432576	34	0.199998805071	–0.153579329326
7	0.050370069425	–0.060246553626	35	0.205924695592	–0.157036098796
8	0.054814487316	–0.062715674677	36	0.211850586112	–0.162468165107
9	0.059752729416	–0.065678619937	37	0.216788828213	–0.165431110367
10	0.065184795727	–0.069629213617	38	0.223702367153	–0.170863176678
11	0.070123037827	–0.073579807298	39	0.229628257674	–0.173826121938
12	0.075061279928	–0.076048928348	40	0.236541796615	–0.178764364039
13	0.080493346238	–0.079999522028	41	0.241480038715	–0.183702606139
14	0.086419236759	–0.082962467289	42	0.245430632396	–0.187159375610
15	0.092838951490	–0.087406885179	43	0.249875050286	–0.191109969290
16	0.098764842010	–0.092345127280	44	0.255307116597	–0.195554387180
17	0.102715435691	–0.095308072540	45	0.262220655537	–0.200986453491
18	0.109135150421	–0.099752490430	46	0.267652721848	–0.205924695592
19	0.113579568312	–0.101233963061	47	0.273578612369	–0.211356761902
20	0.118517810412	–0.103703084111	48	0.279504502889	–0.217776476633
21	0.121480755673	–0.106666029371	49	0.284936569200	–0.222714718733
22	0.127406646193	–0.110122798842	50	0.292343932351	–0.229134433464
23	0.132344888294	–0.113579568312	51	0.297775998661	–0.235060323985
24	0.140246075655	–0.117530161992	52	0.303701889182	–0.240986214505
25	0.146171966175	–0.122468404093	53	0.307652482862	–0.247899753446
26	0.152097856696	–0.125925173563	54	0.310615428122	–0.252837995546
27	0.159011395637	–0.130863415664	55	0.313578373383	–0.258270061857
28	0.164443461947	–0.133332536714	56	0.314072197593	–0.265183600798

Coordinates of discrete points which define the contours bounding the subdomains (continued)

No.	x	y	No.	x	y
57	0.315059846013	–0.268640370268	109	0.381750739352	–0.519650054306
58	0.315059846013	–0.273578612369	110	0.383523581512	–0.524657664182
59	0.314072197593	–0.278516854469	111	0.385296423672	–0.529665274058
60	0.311109252333	–0.281973623939	112	0.387069265831	–0.534672883935
61	0.307158658652	–0.285430393410	113	0.388842107991	–0.539680493811
62	0.304689537602	–0.288393338670	114	0.390614950151	–0.544688103687
63	0.300200000000	–0.289300000000	115	0.397034664882	–0.544194279477
64	0.301972842160	–0.294307609876	116	0.400985258562	–0.548144873157
65	0.303745684320	–0.299315219752	117	0.406417324872	–0.555058412098
66	0.305518526479	–0.304322829629	118	0.412343215393	–0.558515181568
67	0.307291368639	–0.309330439505	119	0.416293809074	–0.560984302619
68	0.309064210799	–0.314338049381	120	0.423701172224	–0.562959599459
69	0.310837052959	–0.319345659257	121	0.428639414325	–0.563947247879
70	0.312609895119	–0.324353269134	122	0.436046777476	–0.563453423669
71	0.314382737279	–0.329360879010	123	0.442960316416	–0.561971951039
72	0.316155579438	–0.334368488886	124	0.449873855357	–0.563453423669
73	0.317928421598	–0.339376098762	125	0.457775042718	–0.562465775249
74	0.319701263758	–0.344383708638	126	0.465182405869	–0.562959599459
75	0.321474105918	–0.349391318515	127	0.472095944809	–0.561478126829
76	0.323246948078	–0.354398928391	128	0.480984780590	–0.560984302619
77	0.325019790238	–0.359406538267	129	0.491355089001	–0.560490478409
78	0.326792632397	–0.364414148143	130	0.504194518463	–0.558515181568
79	0.328565474557	–0.369421758019	131	0.516540123714	–0.556539884728
80	0.330338316717	–0.374429367896	132	0.529379553175	–0.556046060518
81	0.332111158877	–0.379436977772	133	0.538268388956	–0.554070763678
82	0.333884001037	–0.384444587648	134	0.546663400527	–0.553576939468
83	0.335656843196	–0.389452197524	135	0.555058412098	–0.551601642628
84	0.337429685356	–0.394459807401	136	0.567897841559	–0.550120169998
85	0.339202527516	–0.399467417277	137	0.579749622601	–0.548638697367
86	0.340975369676	–0.404475027153	138	0.592589052062	–0.546663400527
87	0.342748211836	–0.409482637029	139	0.603947008893	–0.544194279477
88	0.344521053996	–0.414490246905	140	0.616292614144	–0.540737510007
89	0.346293896155	–0.419497856782	141	0.625675274135	–0.538268388956
90	0.348066738315	–0.424505466658	142	0.639008527807	–0.536786916326
91	0.349839580475	–0.429513076534	143	0.647403539378	–0.533330146856
92	0.351612422635	–0.434520686410	144	0.658761496209	–0.529873377385
93	0.353385264795	–0.439528296286	145	0.670119453040	–0.525428959495
94	0.355158106955	–0.444535906163	146	0.681971234081	–0.520984541604
95	0.356930949114	–0.449543516039	147	0.692341542492	–0.517033947924
96	0.358703791274	–0.454551125915	148	0.704687147744	–0.512589530034
97	0.360476633434	–0.459558735791	149	0.713575983525	–0.509132760563
98	0.362249475594	–0.464566345668	150	0.726909237196	–0.503206870043
99	0.364022317754	–0.469573955544	151	0.737279545607	–0.498268627942
100	0.365795159913	–0.474581565420	152	0.747649854018	–0.492342737421
101	0.367568002073	–0.479589175296	153	0.759501635059	–0.486416846901
102	0.369340844233	–0.484596785172	154	0.769378119260	–0.479009483750
103	0.371113686393	–0.489604395049	155	0.779254603461	–0.473083593229
104	0.372886528553	–0.494612004925	156	0.788637263452	–0.465676230079
105	0.374659370713	–0.499619614801	157	0.800489044494	–0.456787394298
106	0.376432212872	–0.504627224677	158	0.809871704485	–0.449380031147
107	0.378205055032	–0.509634834553	159	0.820735837106	–0.440985019576
108	0.379977897192	–0.514642444430	160	0.829130848677	–0.433083832215

Coordinates of discrete points which define the contours bounding the subdomains (continued)

No.	x	y	No.	x	y
161	0.835550563407	–0.425676469065	213	0.978720469533	–0.034328116622
162	0.842957926558	–0.418269105914	214	0.968834206635	–0.034391678154
163	0.849871465499	–0.410367918553	215	0.958947943736	–0.034455239686
164	0.854809707599	–0.403454379612	216	0.949061680838	–0.034518801218
165	0.861229422330	–0.395553192251	217	0.939175417940	–0.034582362750
166	0.865180016010	–0.390614950151	218	0.929289155042	–0.034645924282
167	0.871599730741	–0.384689059630	219	0.919402892143	–0.034709485814
168	0.879500918102	–0.373824927009	220	0.909516629245	–0.034773047346
169	0.887402105463	–0.363454618598	221	0.899630366347	–0.034836608878
170	0.895797117034	–0.352096661767	222	0.889744103449	–0.034900170410
171	0.902216831764	–0.342220177566	223	0.879857840550	–0.034963731942
172	0.910118019125	–0.331849869155	224	0.869971577652	–0.035027293474
173	0.918019206486	–0.321973384954	225	0.860085314754	–0.035090855006
174	0.924932745427	–0.311603076543	226	0.850199051856	–0.035154416538
175	0.930858635947	–0.302714240762	227	0.840312788957	–0.035217978070
176	0.938265999098	–0.294813053401	228	0.830426526059	–0.035281539602
177	0.945179538039	–0.286911866040	229	0.820540263161	–0.035345101134
178	0.952093076980	–0.277529206049	230	0.810654000263	–0.035408662666
179	0.957525143290	–0.270121842898	231	0.800767737364	–0.035472224198
180	0.964438682231	–0.263208303958	232	0.790881474466	–0.035535785730
181	0.970364572751	–0.255800940807	233	0.780995211568	–0.035599347262
182	0.973821342222	–0.248393577656	234	0.771108948670	–0.035662908794
183	0.973821342222	–0.248393577656	235	0.761222685771	–0.035726470325
184	0.972339869592	–0.238517093455	236	0.751336422873	–0.035790031857
185	0.972339869592	–0.238517093455	237	0.741450159975	–0.035853593389
186	0.976784287482	–0.231603554514	238	0.731563897077	–0.035917154921
187	0.983204002213	–0.224196191363	239	0.721677634178	–0.035980716453
188	0.987154595893	–0.218270300843	240	0.711791371280	–0.036044277985
189	0.990611365364	–0.208887640852	241	0.701905108382	–0.036107839517
190	0.996043431674	–0.199504980861	242	0.692018845484	–0.036171401049
191	0.999994025355	–0.191603793500	243	0.682132582585	–0.036234962581
192	1.003450794825	–0.183208781929	244	0.672246319687	–0.036298524113
193	1.005426091665	–0.175307594568	245	0.662360056789	–0.036362085645
194	1.008389036925	–0.166418758787	246	0.652473793890	–0.036425647177
195	1.010364333766	–0.156542274586	247	0.642587530992	–0.036489208709
196	1.015302575866	–0.146665790385	248	0.632701268094	–0.036552770241
197	1.019746993757	–0.134814009344	249	0.622815005196	–0.036616331773
198	1.023697587437	–0.120986931463	250	0.612928742297	–0.036679893305
199	1.024191411647	–0.111604271472	251	0.603042479399	–0.036743454837
200	1.023697587437	–0.103703084111	252	0.593156216501	–0.036807016369
201	1.024191411647	–0.092838951490	253	0.583269953603	–0.036870577901
202	1.024191411647	–0.082468643079	254	0.573383690704	–0.036934139433
203	1.024685235857	–0.075061279928	255	0.563497427806	–0.036997700965
204	1.023697587437	–0.066666268357	256	0.553611164908	–0.037061262497
205	1.022216114807	–0.058271256786	257	0.543724902010	–0.037124824029
206	1.018265521126	–0.050370069425	258	0.533838639111	–0.037188385561
207	1.016290224286	–0.042962706274	259	0.523952376213	–0.037251947093
208	1.017277872706	–0.037530639964	260	0.514066113315	–0.037315508625
209	1.018265521126	–0.034073870494	261	0.504179850417	–0.037379070157
210	1.008379258228	–0.034137432026	262	0.494293587518	–0.037442631689
211	0.998492995329	–0.034200993558	263	0.484407324620	–0.037506193221
212	0.988606732431	–0.034264555090	264	0.474521061722	–0.037569754753

Coordinates of discrete points which define the contours bounding the subdomains (continued)

No.	x	y	No.	x	y
265	0.464634798824	–0.037633316285	288	0.237250752164	–0.039095231520
266	0.454748535925	–0.037696877817	289	0.227364489265	–0.039158793052
267	0.444862273027	–0.037760439349	290	0.217478226367	–0.039222354584
268	0.434976010129	–0.037824000881	291	0.207591963469	–0.039285916116
269	0.425089747231	–0.037887562413	292	0.197705700571	–0.039349477648
270	0.415203484332	–0.037951123945	293	0.187819437672	–0.039413039180
271	0.405317221434	–0.038014685477	294	0.177933174774	–0.039476600712
272	0.395430958536	–0.038078247009	295	0.168046911876	–0.039540162244
273	0.385544695638	–0.038141808541	296	0.158160648978	–0.039603723776
274	0.375658432739	–0.038205370073	297	0.148274386079	–0.039667285308
275	0.365772169841	–0.038268931605	298	0.138388123181	–0.039730846840
276	0.355885906943	–0.038332493137	299	0.128501860283	–0.039794408372
277	0.345999644044	–0.038396054669	300	0.118615597385	–0.039857969904
278	0.336113381146	–0.038459616201	301	0.108729334486	–0.039921531436
279	0.326227118248	–0.038523177733	302	0.098843071588	–0.039985092968
280	0.316340855350	–0.038586739265	303	0.088956808690	–0.040048654500
281	0.306454592451	–0.038650300797	304	0.079070545792	–0.040112216032
282	0.296568329553	–0.038713862329	305	0.069184282893	–0.040175777564
283	0.286682066655	–0.038777423861	306	0.059298019995	–0.040239339096
284	0.276795803757	–0.038840985393	307	0.049411757097	–0.040302900628
285	0.266909540858	–0.038904546924	308	0.039525494199	–0.040366462160
286	0.257023277960	–0.038968108456	309	0.029639231300	–0.040430023692
287	0.247137015062	–0.039031669988	310	0.019752968402	–0.040493585224